The electrical transport properties of bulk nitrogen doped carbon microspheres

W P Wright[1,2], V D Marsicano[1,2], J M Keartland[1,2], R M Erasmus[1,2], S Dube[2,3] and N J Coville[2,3]

[1] School of Physics, University of the Witwatersrand, P.O. Wits, 2050 Johannesburg, South Africa

[2] DST-NRF Centre of Excellence in Strong Materials, P.O. Wits, 2050 Johannesburg, South Africa

[3] Molecular Sciences Institute and School of Chemistry, University of the Witwatersrand, P.O. Wits, 2050 Johannesburg, South Africa

E-mail: keartland@psi.phys.wits.ac.za

Abstract. Bulk nitrogen-doped carbon microspheres were synthesised using a horizontal chemical vapour deposition reactor (h-CVD). The sample was characterized using scanning electron microscopy (SEM), Raman spectroscopy and electron paramagnetic resonance (EPR) spectroscopy. Characterization showed spherical graphitic carbon microparticles with nitrogen incorporation in the lattice structure, and diameters ranging from 2.6 μm to 750 nm. EPR spectroscopy was also used as a non-destructive technique to measure the percentage of substitutional nitrogen present in the sample. This was determined to be 3.4 %. Electrical transport measurements were performed on the sample and resistance measurements show clear semiconducting behaviour from room temperature down to 10 K. The IV characteristics display curves with increasing non-linearity as temperature decreases. An anomaly is present in the IV characteristics at 300 K. A number of models were used to explain the data and the one providing the best fit is fluctuation induced tunneling. The model provides a satisfactory description of the data for both the IV characteristics and the resistance measurements.

1. Introduction

Since the discovery of carbon nanotubes (CNT) in 1991 [1], carbon nanomaterials have received intense and ongoing interest. In recent years another novel carbon allotrope has received much attention, the carbon microsphere (CMS). This attention is in no small part due to their unique physical properties, including great structural stability which has prompted their usage as a strengthening additive in materials such as rubber. Other uses for CMSs are as a gas storage material [2] and as anode materials in Lithium-Ion batteries [3].

The synthesis of CMSs using the chemical vapour deposition (CVD) technique has been widely reported in the literature [4], [5], [6]. Samples have been synthesised using a wide variety of furnace parameters, gas flow rates and precursors in an attempt to obtain a set of optimal growth conditions. The CVD technique is advantageous because a catalyst is not required. This ensures high sample purity and ease of synthesis and characterization of doped samples of CMSs. Doping can be achieved by allowing a dopant containing additive to flow in the reactor along with the carbon source.

Previously it has been shown that the doping of CNTs with nitrogen leads to n-type semiconducting behaviour [7] whereas doping with boron leads to p-type semiconducting behaviour [8]. The synthesis and physical properties of boron doped CMSs have been described previously [9]. Electrical transport measurements show that undoped CMSs conduct via Mott Variable Range Hopping [10], the boron doped samples adhered to this model of conduction only at temperatures higher than 170 K and exhibited a much lower conductivity than the undoped sample. This reduction in conductivity has been attributed to charge localization [9]. It has also been shown that CMSs exhibit a Curie type paramagnetism that has been attributed to their characteristic architecture [11].

In this paper we detail the synthesis process of a sample of nitrogen doped CMSs using the CVD technique. The sample was then characterized using scanning electron microscopy, Raman and electron paramagnetic resonance (EPR) spectroscopy. EPR spectroscopy was also used to determine the nitrogen content of the sample. Temperature dependent resistance measurements and IV characteristics were performed on the sample, to explore the underlying conduction mechanism at work in the sample.

2. Synthesis

Samples were synthesized in a horizontal CVD reactor via the pyrolysis of acetylene as is seen elsewhere [12]. The acetylene was introduced into the reactor by using argon as a carrier gas. Reactants were introduced after the furnace was allowed to reach a temperature of 850 °C and was set to a flow rate of 100ml/min. The source of nitrogen dopant, acetonitrile, was then allowed to flow with the carrier gas. The reaction was left to run for 2 hours. Other runs were performed where the temperature was increased to 900 °C. Once the reaction was complete, samples were collected from the quartz boat in the centre of the reactor and from the lining of the quartz tube forming the interior of the reactor. The sample used in the remainder of this research was collected from the middle of the quartz tube. The other samples collected, 5 in total, would be used to determine the nitrogen content of the spheres.

3. Characterization

3.1. Scanning Electron Microscopy

Figure 1 shows the electron microscope images that were taken of the sample with a Topcon SM510 Scanning Electron Microscope. At lower magnifications of approximately 500× (Figure 1a), larger agglomerates of particles can clearly be seen. The particles have a tendency to chain together forming long chains and groups of particles. Higher magnification images of approximately 5000× (Figure 1b) clearly show the spherical shape of the constituent particles. Analysis of the sizes of the particles across different sites in the sample show a large distribution in measured diameters for the spheres. The largest measured sphere diameters are approximately 2.6 μm. The smallest measured sphere diameters are approximately 750 nm.

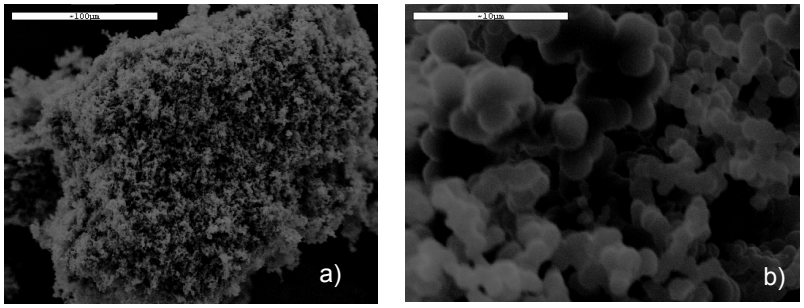

Figure 1. SEM images of the sample: a) 500× b) 5000×

3.2. Raman Spectroscopy

Raman spectroscopy measurements were performed using 514 nm and 647 nm laser light sources in order to probe the structural properties of the synthesized product. Major peaks were observed at 1381 cm^{-1} and 1595 cm^{-1} with a minor peak at approximately 1200 cm^{-1}.The two dominant spectral lines, known as the D and G bands, indicate the presence of a graphitic carbon structure [13].

3.3. Electron Paramagnetic Resonance Spectroscopy

The EPR spectrum for the nitrogen-doped carbon spheres was acquired using a Bruker ESP 300E spectrometer in continuous wave mode in order to search for magnetic impurities which would be indicative of nitrogen incorporation in the graphitic lattice. The observed spectra are characteristic of pristine CMSs [14] as well as doped CNTs [15]. The resonance signal is slightly Dysonian indicating the presence of conduction electrons [16].

A novel technique was developed to determine the nitrogen concentration of the sample using the EPR spectra. Spectra of a set of carbon spheres produced with similar conditions but with different nitrogen concentrations were collected. The spin concentration (EPR spectrum amplitude divided by the sample mass) provides a rudimentary calibration curve for the spectrometer. When applied to this calibration curve the sample showed a nitrogen concentration of 3.4 % with an error of 0.7 %. The errors are large due to the small size of the sample used and the difficulties associated with spin-concentration EPR experiments.

4. Electrical Transport Measurements

Four-probe resistance measurements were performed on the sample over the temperature range of 300 K to 10 K using a Fluke 8840A digital multimeter operating in resistance mode. A constant current of 100 μA was used to take resistance measurements. The CMS powder was compacted into a sample holding cell using a hand press. Electrical contact was made with the sample through nickel needles acting as pressure contacts. Low temperature measurements were performed using an Oxford continuous flow cryostat. An accurate measure of the sample temperature was obtained using a carbon glass resistance thermometer mounted near the sample at the base of the cryostat.

Variable temperature IV characteristics were measured using a home-built digital variable power supply. This power supply was constructed using a conventional laboratory desktop 30 V DC power supply and an ATMEL ATmega328 microcontroller loaded with the Arduino open source development platform boot loader. This power supply could provide voltages from 0 V-30 V in steps of 500 mV for high bias measurements. The sample for the IV characteristics measurements was prepared in the same way as in the resistance measurements. The voltage drop across the sample was measured using a Fluke 8840A digital multimeter and the current flowing through the sample was measured using an HP 34401A digital multimeter.

4.1. Resistance Measurements

Three different models were used to try account for the data obtained from the resistance. Mott variable range hopping (Mott VRH), where electrons traverse the material by hopping from different localized impurity states; Efros-Shklovskii variable range hopping (ES VRH), where a Coulomb gap forms as the density of states vanishes at the Fermi level; and fluctuation induced tunnelling (FIT), where the material is modelled as a series of metallic regions with small barriers separating them. Electrons are able to either travel over the barriers at higher temperatures, or tunnel through them at lower temperatures. This mechanism is important in describing conduction across junctions between CNTs. These models were chosen as they have found success in modelling the resistance and resistivity data obtained for a wide variety of

Table 1. Parameters extracted from the FIT model fit to the resistance data

T_b	T_s	β
250 ± 30	40 ± 4	1.2 ± 0.2

both bulk and individual examples of nanostructures. Some examples include CNT mats, both doped [17] and pristine [18] and conducting polymer nanofibers [19].

Both Mott VRH and ES VRH can be described by an equation of the form:

$$R(T) = R_0 e^{\left(\frac{T_0}{T}\right)^{\frac{1}{d+1}}} \tag{1}$$

where T_0 is the characteristic temperature, d is the dimensionality of the system and in the case of 3 dimensions, Mott VRH is given by $d = 3$ and, in the case of ES VRH, is given by $d = 1$. R_0 is a constant which contains information regarding the localization length in the case of ES VRH and information regarding the density of states at the Fermi level in the case of Mott VRH.

The FIT model can be described by an equation of the form:

$$R(T) = \beta e^{\left(\frac{T_b}{T_s + T}\right)} \tag{2}$$

where β is a weak function of temperature that contains information regarding the barrier height and other properties of the network structure of connecting microparticles. It can be taken as a constant compared to the temperature dependence of the exponential. T_s is the temperature above which thermal fluctuations become a competing factor. T_b is a much more complicated quantity which is dependent on the barrier shape and height and is affected by the local electric field and the image force (image charges present in the metal contacts)[17]. It relates to the temperature below which tunnelling through the potential barriers is the dominant conduction mechanism.

Figure 2 shows each of the above equations fitted to the reduced resistance data (resistance at a given temperature over the resistance at 300 K) obtained for the sample. It can clearly be seen that the FIT model describes the data the most accurately. By analysing the parameters of the fit, we are able to extract the values of T_b, T_s and β. These values are given in Table 1 along with their associated errors. The values obtained are consistent with those found in the literature [17], [20], [21]. The uncertainties in the values for T_s and T_b are quite large and it has been hypothesized that this can be attributed to the wide variety of type and number of junctions between interconnecting microparticles [17]. The spherical nature of the microparticles increases the potential for different kinds of contacts between the microparticles. In the experiments described here, the temperatures studied did not approach the value of T_s. This indicates that thermal fluctuations play a significant role in allowing electrons to traverse the barriers between metallic regions. The T_b values are higher than those obtained for Nitrogen doped CNTs [17] which is indicative of a higher barrier height between conducting regions.

4.2. IV Characteristics

The temperature range investigated was between 300 K and 100 K in steps of 40 K. The voltage range over which readings were taken was between 0 V and 24 V at each temperature step. In the temperature range of 260 K to 100 K a clear trend can be seen in terms of the linearity of the IV characteristics. At higher temperatures the linear component dominates. As the temperature is decreased, the IV characteristics become more nonlinear. This trend provides further evidence that fluctuation induced tunnelling is the dominate mechanism for electrical

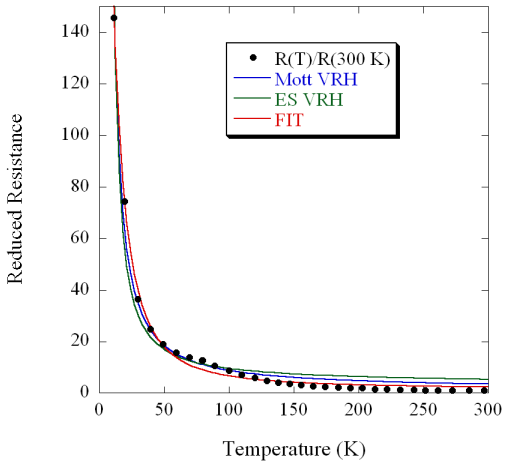

Figure 2. Model fits to resistance data. Clear semiconducting behaviour can be seen. While all 3 models provide a credible description of the data, it is clear that fluctuation induced tunneling provides the best.

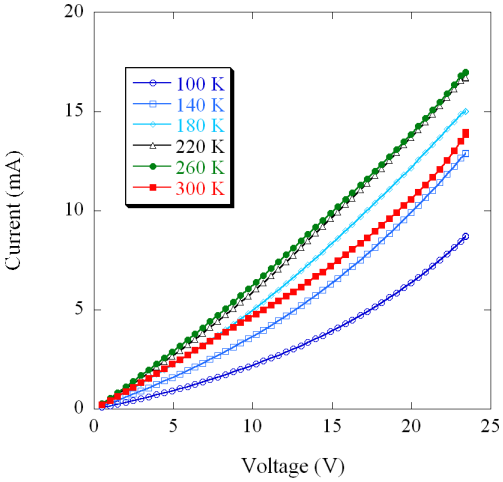

Figure 3. Fluctuation induced tunneling model fit to variable temperature IV characteristics. A Clear increase in non-linearity of the curves can be seen with decreasing temperature providing further evidence of fluctuation induced tunneling being the dominant conduction mechanism.

Table 2. Parameters extracted from the FIT model fit to the IV characteristics

	100 K	140 K	180 K	220 K	260 K	300 K
G_0 (in mS)	0.15	0.26	0.41	0.51	0.55	0.55
V_0 (in V)	26	26	35	37	51	−67
h	0.001	0.114	0.245	0.36	0.36	0.87

transport in this temperature range. The behaviour of linearly dominated IV characteristics at higher temperatures is indicative of carriers being assisted by thermal fluctuations to travel over the potential barriers. The behaviour of nonlinear dominated IV characteristics at lower temperatures and an increase in nonlinearity as temperature is decreased is indicative of the carriers not having enough thermal energy to surmount the potential barriers and they tunnel through them.

Using the expression modified by Kaiser [19], the IV characteristics of a system where fluctuation induced tunnelling is the dominant transport mechanism is given by:

$$G = \frac{I}{V} = G_0 \frac{e^{\left(\frac{V}{V_0}\right)}}{1 + h\left(e^{\frac{V}{V_0}} - 1\right)} \tag{3}$$

where G_0 is the temperature dependent low field conductance, h is the parameter which governs the slowing of exponential increase at higher field values and V_0, which has a strong dependence on the potential barrier height, is the voltage scaling factor.

Figure 3 shows the fits of the above equation to the IV data over the entire temperature range. The parameters of the fits are given in Table 2. In the temperature range 100 K to

260 K, the model fits the data very well and the parameters obtained correspond well with and follow the same trend as those seen in the literature [22]. The correspondence between the resistance data and the IV characteristics of the sample in this temperature range gives a strong indication that fluctuation induced tunnelling is indeed the dominant conduction mechanism for this sample. However, the IV curve at 300 K is atypical. It already has a nonlinear component to it and when an attempt was made to fit the model to the data, a poor fit was obtained when compared to the other temperatures and non-physical parameters were extracted. This leads us to believe that another mechanism is competing with FIT at temperatures comparable to 300 K. High temperature measurements would be useful in exploring the reasons for this behaviour.

5. Conclusion

A sample of nitrogen-doped CMSs were synthesised using the CVD technique. The samples were characterized using electron microscopy confirming the spherical nature of the nanomaterials. Raman spectroscopy confirmed the graphitic nature of the samples, and EPR spectroscopy measurements indicated that nitrogen is incorporated into the lattice as a substitutional impurity. Electrical transport measurements were performed on the sample and it was found from the resistance measurements that the sample conducts via fluctuation induced tunnelling in the temperature range of 300 K to 10 K. The model fit parameters corresponded to those found in the literature. The IV characteristics measurements of the sample confirmed that fluctuation induced tunnelling is the dominant conduction mechanism in the temperature range 260 K to 100 K. An anomaly was discovered in the 300 K IV curve. Higher temperature experiments will allow us to investigate this effect.

References

[1] Iijima S 1991 *Lett. Nature.* **354** 56
[2] Wu C, Zhu X, Ye L, Yang C, Hu S, Lei L and Xie Y 2006 *Inorg. Chem.* **45**
[3] Wang Y, Su F, Wood C, Lee J and Zhao X 2008 *Ind. Eng. Chem. Research.* **47** 2294–300
[4] Wang Z and Yin J 1998 *Chem. Phys. Lett.* **289** 189–192
[5] Mehraban Z, Farzaneh F and Dadmehr V 2009 *Mat. Lett.* **63** 1653–1655
[6] Miao J, Hwang D, Narasimhulu K, Lin P, Chen Y, Lin S and Hwang L 2004 *Carbon.* **42** 813–822
[7] Ewels C and Glerup M 2005 *J. Nanosci. and Nanotech.* **5** 1345–1363
[8] Mondal K, Strydom A, Erasmus R, Keartland J and Coville N 2008 *Mat. Chem. and Phys.* **111** 386–390
[9] Mondal K, Strydom A, Tetana Z, Mhlanga S, Witcomb M, Havel J, R R E and Coville N 2009 *Mat. Chem. and Phys.* **114** 973–977
[10] Romanenko A, Anikeeva O, Okotrub A, Bulusheva L, Kuznetsov V, Butenko Y, Chuvilin A, Dong C and Ni Y 2002 *Phys. Sol. Stat.* **44** 487–489
[11] Calderon-Moreno J, Labarta A, Batlle X, Pradell T, Crespo D and Binh V 2007 *Chem. Phys. Lett.* **447** 295–299
[12] Aili M, Xiaomin W, Tianbao L, Xuguang L and Bingshe X 2007 *Mat. Sci. Eng. A* **443** 54–59
[13] Tuinstra F 1970 *J. Chem. Phys.* **53** 1126
[14] Pol V 2010 *Environ. Sci. Technol.* **44** 4753–?4759
[15] Hsu W, Chu S, Firth S *et al.* 2000 *Chem. Phys. Lett.* **323** 572–579
[16] Dyson F 1958 *Phys. Rev.* **98** 349–359
[17] Barnes T, Blackburn J, Lagemaat J, Coutts T, and Heben M 2008 *ACS. Nano.* **2** 1968–1976
[18] Bekyarova E, Itkis M, Cabrera N, Zhao B, Yu A, Gao J and Haddon R 2005 *J. Amer. Chem. Soc.* **127** 5990–5995
[19] Kaiser A, Rogers S and Park Y 2004 *Mole. Crys. Liq. Crys.* **415** 115–124
[20] Sheng P 1980 *Phys. Rev. B* **21** 2180–2195
[21] Shiraishi M and Ata M 2002 *Synth. Metal.* **128** 235–239
[22] Long Y, Yin Z, Li M, Gu C, Duvail J, Jin A and Wan M 2009 *Chinese. Phys. B* **18** 2514–2522